Sensors and Materials, Vol. 38, No. 6 (2026) 3287–3300
MYU Tokyo

S & M 4503

Establishing a 3D Balance Assessment Norm for Older Adults Based on Multifactor Grey Relational Analysis of Force Platform Data

Chih Sheng Chang* and Ke Shin Chong

Department of Product and Media Design, Fo Guang University,
No. 160, Linwei Road, Jiaoxi Township, Yilan County 26247, Taiwan.

(Received January 13, 2026; accepted May 26, 2026)

Keywords: ground reaction force, sit-to-stand task, geriatric balance, fall risk, balance assessment

The objective of this study was to establish a quantitative balance assessment model for older adults by integrating high-frequency force platform sensor data with grey relational analysis to evaluate morphological similarity. Utilizing a 1000 Hz sampling rate, we extracted seven temporal and five weight-related balance factors during sit-to-stand tasks. Data were collected from 60 participants, including 22 healthy young adults—serving as a normative baseline—and 38 older adults. On the basis of these seven time factors, five weight factors, and clinical indicators derived from the Berg Balance Scale and body mass index, three 2D balance assessment standards were formulated, subsequently leading to the derivation of a comprehensive 3D assessment norm. This 3D assessment norm visualizes individual balance performance through specific functional quadrants and may help identify possible compensatory adaptations and functional differences that traditional scales may overlook. The results suggest that the proposed 3D assessment norm provides a standardized visual platform for characterizing individual balance performance and may support future validation-oriented studies and AI-assisted support systems.

1. Introduction

Population aging has emerged as a significant global demographic phenomenon with projections indicating that the world's population will reach 9.7 billion by 2050. This demographic shift presents unprecedented challenges to healthcare systems, particularly regarding fall-related injuries among older adults.(1) Statistics reveal that fatal falls incur direct medical expenses exceeding $50 billion annually, while nonfatal falls account for hundreds of millions in additional healthcare costs.(2) Beyond the economic burden, falls often result in severe fractures and head injuries, leading to a "vicious cycle" of bed confinement, organ failure, and high mortality rates. Consequently, maintaining postural balance is not merely a functional requirement but a critical factor in preserving independence in the aging population.

In clinical settings, observational performance tests such as the Berg balance scale (*BBS*) and the Tinetti Gait and Balance Assessment remain the primary tools for fall risk screening.(3,4)

*Corresponding author: e-mail: cschang@mail.fgu.edu.tw
https://doi.org/10.18494/SAM6171

ISSN 0914-4935

However, these tools are often criticized for their inherent subjectivity and the "ceiling effect".[5] High-functioning older adults may receive identical scores despite adopting different strategies to maintain stability.[6] Traditional scales often fail to capture subtle biomechanical differences during complex movements, leading to limited sensitivity in detecting early functional changes.[7] To address these limitations, objective assessments using high-frequency force platform data have become important for quantifying balance performance beyond simple visual observation.

Among various functional movements, the sit-to-stand (STS) task is recognized as one of the most demanding transitions for older adults, requiring the precise coordination of temporal and force-related variables.[8] While the analysis of STS performance has attempted in previous sensor-based studies, many rely on isolated parameters such as total duration or peak force. Such simplified metrics often overlook the intricate relationship between phase-specific timing and the magnitude of force distribution.[9] A comprehensive understanding of balance strategies requires a multidimensional analysis of factors captured at high sampling rates (e.g., 1000 Hz) to ensure the reliability of the derived physiological characteristics.[10]

To address the complexity of multifactor balance data, in this study, we introduce grey relational analysis (GRA) as a reference-based evaluation framework. GRA is suitable for analyzing biological signals that exhibit high inter-individual variability and uncertainty.[11] The methodological core of this research involves a hierarchical formulation of balance standards: by extracting seven temporal factors and five weight-related factors, three distinct 2D balance assessment standards were first established. These 2D standards were subsequently integrated to derive a comprehensive 3D assessment norm. By mapping 60 participants—38 older adults and 22 healthy young adults—into this 3D functional space, we provide a visual framework for characterizing individual functional differences in balance-related performance. This approach may help improve the interpretation of functional differences and provide a basis for future assessment-oriented applications.

2. Methods

2.1 Participants

A total of 60 participants were enrolled in this study, consisting of a healthy young group (n = 22) and an older adult group (n = 38). All participants provided written informed consent before the experiment, and the study protocol was conducted in accordance with the ethical standards of the local Institutional Review Board.

The healthy young group, serving as the normative baseline, comprised university students with no history of musculoskeletal or balance impairments. For the older adult group, a total of 62 individuals aged 65 or older were initially recruited from local community centers. To ensure the integrity of the high-frequency (1000 Hz) sensor data and the robustness of the 3D assessment norm, a rigorous screening process was implemented. As a result, 24 participants were excluded on the basis of the following criteria: (1) inability to maintain a stable standing posture before starting the STS movement (n = 11); (2) technical errors or signal clipping in the force platform

data during high-speed sampling (n = 8); and (3) incomplete clinical assessment records, such as *BBS* or body mass index (*BMI*) data (n = 5).

Consequently, 38 qualified older adult participants (average age 70.4 ± 4.3 years) were finalized for analysis. The demographic and clinical characteristics of all the participants, including age, height, weight, *BMI*, and *BBS* scores, were also documented.

2.2 Experimental setup and instrumentation

Vertical ground reaction forces (VGRFs) were measured using two high-precision 500 × 500 mm force platforms (accuracy: 0.20 N), each integrated with four strain-gauge load cells. To ensure postural stability and ergonomic consistency across a diverse range of participants (38 older adults and 22 young adults), a customized ergonomic chair was developed on the basis of American National Standards Institute (ANSI) and Chinese National (GB) Standards.

Following ANSI guidelines, the seat plane was inclined 4° backward, with a 100° angle maintained between the seat and backrest. The seat featured a width of 45 cm and a depth of 40 cm, with an adjustable height ranging from 32 to 46 cm to accommodate the individual anthropometric variations of the participants as per GB standards.

The VGRF signals from the platforms were defined as the force applied to the ground or chair during the transition. These signals were captured and processed using a 16-bit analog-to-digital (A/D) converter (NI PCI-6220, National Instruments) combined with multichannel signal amplifiers. Data were simultaneously recorded on a PC at a high sampling frequency of 1000 Hz, providing the necessary temporal resolution for the subsequent multifactor GRA.

2.3 Measurements

VGRFs were characterized by two primary curves: curve B for the force applied through the buttocks and curve L for that through the legs. Curve T was derived as the sum of B and L, representing the total body force during the STS transition. To ensure signal reliability and temporal resolution, data were sampled at 1000 Hz and subsequently smoothed using a symmetric 100-point moving average filter (100 ms window) to suppress high-frequency electrical noise while preserving the morphological integrity of the VGRF curves prior to quantitative analysis.

The critical events of the STS maneuver were identified as follows: the onsets (B_s, L_s, T_s) were defined as the first nonzero difference from the baseline after the action cue. Seat-off was precisely defined as the point where curve B reached zero (B_0), indicating the moment of loss of contact with the chair. The peak and lowest forces (T_p, L_p, T_{pw}, L_{pw}) were captured during the transition, and the STS task was considered complete when curve T equaled the participant's body weight. By calculating the time intervals between these sequential events and extracting the specific force magnitudes, 12 core biomechanical factors—consisting of seven temporal and five weight-related measures—were extracted for subsequent analysis. Additionally, clinical parameters including the *BBS* and *BMI* were integrated to provide a comprehensive functional profile, as detailed in Table 1. As illustrated in Fig. 1, the VGRF curves (B, L, and T) and key points (B_s, T_p, and *seat-off*) were defined to extract temporal and weight-related factors.

Table 1
Time, weight, and other balance factors.

Category	No.	Factor	Explanation
Time factors	1	$B_s - T_p$	Duration between B_s and T_p
	2	$B_s - L_p$	Duration between B_s and L_p
	3	$B_s - seat\text{-}off$	Duration between B_s and *seat-off*
	4	$B_s - end$	Duration between B_s and *end*
	5	$T_p - L_p$	Duration between T_p and L_p
	6	$T_p - seat\text{-}off$	Duration between T_p and *seat-off*
	7	$L_p - seat\text{-}off$	Duration between L_p and *seat-off*
Weight factors	1	T_{pw}	Maximum ground reaction force of Curve T
	2	L_{pw}	Maximum ground reaction force of Curve L
	3	T_{minw}	Minimum body force during the ascending phase
	4	$T_{pw} - T_{minw}$	Force difference between T_{pw} and T_{minw}
	5	$L_{pw} - T_{minw}$	Force difference between L_{pw} and T_{minw}
Additional factors	1	*BBS*	Berg Balance Scale score
	2	*BMI*	Body Mass Index value

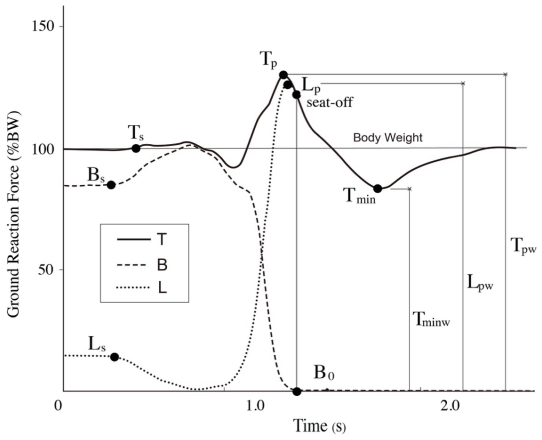

Fig. 1. GRF parameters and time course of STS movement.

2.4 GRA application

In accordance with the grey system theory, GRA is employed for system modeling under uncertainty, relational analysis, and decision-making, and has been applied in engineering optimization.[12,13] In this study, GRA was used to normalize biomechanical parameters and establish a relationship between the discrete sequences of the older adult group (n = 38) and the healthy young reference group (n = 22). The primary objective of this transformation was to characterize relational structure within the high-frequency force platform data and to reduce the effect of scale differences across variables.[14] In this study, the analytical role of GRA was to evaluate the morphological similarity of sequence curves between each participant and the reference group. By characterizing the dynamic "trends" and "shapes" of movement-related data, GRA provides a reference-based framework for examining subtle functional variations and possible compensatory adaptations in older adults.

To improve comparability across variables with different units, all raw factors were subjected to a dimensionless normalization process prior to calculating the GRA grades, allowing time, weight-related, and clinical variables to be compared within the same GRA framework. The mathematical procedure is described as follows.

(1) Definition of GRA Space:

In GRA space, the set of sequences is denoted by X, where each sequence is expressed as $x_i = (x_i(1), x_i(2), \ldots, x_i(k))$, with $i = 0, 1, 2, \ldots, m$ and $k = 1, 2, \ldots, n \in N$, where

$$x_i = \left(x_i(1), x_i(2), x_i(3), \ldots, x_i(k)\right). \tag{1}$$

According to grey system theory, one sequence is selected as the reference sequence, whereas the remaining sequences are treated as comparison sequences. In this study, Nagai's GRA grade was used, as shown in Eq. (2).[15]

(2) Calculation of Nagai's GRA Grade:

$$\Gamma_{0i} = \Gamma(x_0(k), x_i(k)) = \frac{\overline{\Delta}_{max.} - \overline{\Delta}_{0i}}{\overline{\Delta}_{max.} - \overline{\Delta}_{min.}},\ \overline{\Delta}_{0i} = \sqrt{\sum_{k=1}^{n}\left[\Delta_{0i}(k)\right]^2} \tag{2}$$

where $i = 0, 1, 2, \ldots, m$, $k = 1, 2, \ldots, n$

x_0 is standard sequence, x_i are comparison sequences.

$\Delta_{0i} = \left\|x_0(k) - x_i(k)\right\|$: norm between x_0 and x_i. $\overline{\Delta}_{0i}$: mean of Δ_{0i}.

(3) Determination of Maximum and Minimum Differences:

$$\begin{aligned} \Delta_{min.} &= \underset{j\in i}{\overset{min.min.}{\forall}} \forall k \left\|x_0(k) - x_j(k)\right\| \\ \Delta_{max.} &= \underset{j\in i}{\overset{max.max.}{\forall}} \forall k \left\|x_0(k) - x_j(k)\right\| \end{aligned} \tag{3}$$

2.5 Establishment of reference sequences for numerical analysis

To implement the multifactor GRA, a standard reference sequence (x_0) must be established for each of the three assessment dimensions: time factors, weight-related factors, and clinical indicators (*BBS* and *BMI*). In this study, the reference sequences represent the normative baseline derived from the average performance of the healthy younger group ($n = 22$).

The reference sequence for each factor k is calculated as the arithmetic mean of the younger participants' data, as shown in Eq. (4).

$$x_0(k) = \frac{\sum_{i=1}^{N} x_i(k)}{N} \tag{4}$$

Here, $N = 22$ denotes the total number of healthy younger adults, and $x_i(k)$ represents the k-th factor value of the i-th younger participant.

The numerical analysis was conducted across three distinct categories.

(1) Time Factors: A standard sequence was established by averaging the seven temporal performance factors of the healthy group.
(2) Weight Factors: Similarly, a reference sequence was obtained using the average of the five weight-shifting factors.
(3) *BBS* & *BMI* Factors: The normative baseline for clinical performance was derived from the average *BBS* and *BMI* values of the healthy reference group.[16]

In the present framework, the young-group mean values were used to construct the reference sequences for GRA calculation, whereas the minimum GRA grades observed within the young group were used as conservative lower-bound criteria for visual classification. These reference sequences serve as the reference coordinates in the GRA space, against which the 38 older adult participants are compared to derive their respective relational grades across the three dimensions.

3. Results

3.1 Participant characteristics

The health records of community center residents were reviewed to identify suitable participants for the older adult group. Two physical therapists administered clinical assessments, including the *BBS*, Barthel Index (*BI*), Instrumental Activities of Daily Living (*IADL*) scale, and Mini-Mental Status Examination (*MMSE*), to ensure participants possessed sufficient cognitive and physical function for the experiment.

As detailed in Sect. 2.1, 38 older adult participants (average age 70.4 ± 4.3 years) were recruited from an initial pool of 62 candidates based on the following cutoff scores: $BBS \geq 41$, $BI \geq 60$, $MMSE > 17$, and $IADL \geq 7$. In contrast, the healthy young group ($n = 22$, mean age 19.7 ± 0.8 years) achieved maximal scores across all clinical balance and cognitive assessments. Table 2 provides a comprehensive overview of the demographic and clinical characteristics of all 60 participants.

3.2 Establishment of reference lower-bound GRA values

Using the healthy young group as the reference baseline, we calculated the relational grades for time factors, weight factors, and *BBS*/*BMI* factors for all the participants. For the visual classification of balance-related performance in older adults, a conservative lower-bound

Table 2
Demographic and clinical characteristics of participants.

Characteristic		Older adults (n = 38)	Healthy adults (n = 22)
Gender	Male	16	11
	Female	22	11
Anthropometrics	Age (yr)	70.4 ± 4.3	19.7 ± 0.8
	Height (cm)	156.6 ± 8.7	161.9 ± 9.5
	Weight (kg)	62.3 ± 11.8	57.7 ± 9.8
	BMI (kg/m^2)	25.6 ± 5.0	21.9 ± 1.9
Clinical assessments	*BBS* (score)	46.3 ± 3.3	56.0 ± 0.0
	BI (score)	95.2 ± 3.6	100.0 ± 0.0
	MMSE (score)	29.6 ± 1.0	30.0 ± 0.0
	IADL (score)	7.6 ± 0.5	8.0 ± 0.0

criterion was established for each dimension in this study on the basis of the minimum GRA grades observed within the healthy young group. The results showed that the reference lower-bound GRA grade for time factors among healthy adults was 0.9623. In comparison, a substantial portion of the older adult participants exhibited values below this threshold, suggesting reduced movement efficiency. Similarly, the corresponding reference lower-bound values were 0.7999 for weight factors and 0.8856 for the clinical *BBS*/*BMI* factor. These distributions across the time, weight, and *BBS*/*BMI* dimensions [shown in Figs. 2(a)–2(c)] provide the basis for the subsequent 3D assessment norm. The individual GRA grades for all participants are presented in Table 3.

4. Discussion

In this study, we utilized a high-frequency (1000 Hz) force platform system to quantify biomechanical characteristics during the STS transition.[17] An important methodological feature of this research is the inclusion of a healthy younger group (n = 22) as a reference baseline.[18] Through GRA, the performance of each older participant was quantified as a relational grade, representing similarity to the reference performance of the healthy young group. A higher GRA grade (closer to 1.0) may be interpreted as indicating greater similarity to the reference values derived from the healthy young group.

4.1 Interaction between time and weight factors

The interaction between temporal efficiency and weight-shifting power defines four biomechanical clusters based on the GRA thresholds (0.9623 for time and 0.7999 for weight), as illustrated in Fig. 3 and Table 4. Area I (13.2%, 5/38) represents the reference-like cluster, where older adult participants maintain GRA grades closest to the younger benchmark, suggesting relatively preserved neuromuscular coordination.[19] Area II (10.5%, 4/38) represents "Momentum Seekers", who maintain higher temporal efficiency (time ≥ 0.9623) despite reduced weight-shifting power (weight < 0.7999), which may reflect greater reliance on momentum during seat-off. Area III (26.3%, 10/38) identifies the "Dual-Deficit Group," characterized by concurrent reductions in both temporal efficiency and weight-shifting power (time < 0.9623 and

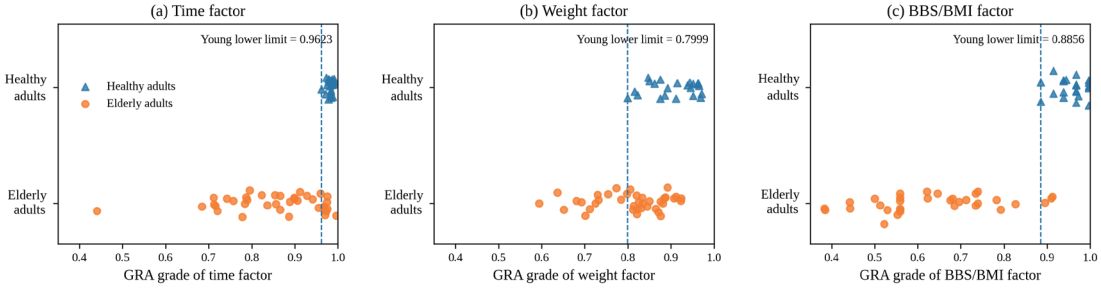

Fig. 2. (Color online) Categorical scatter plots of GRA grade distributions for (a) time factor, (b) weight factor, and (c) *BBS*/*BMI* factor. The y-axis indicates participant group (categorical; no quantitative scale); points are vertically jittered for readability. Dashed vertical lines represent the young (healthy) lower limits (time = 0.9623, weight = 0.7999, *BBS*/*BMI* = 0.8856).

Table 3
GRA grades for each participant. Columns report the GRA grades of time, weight, and *BBS*/*BMI* factors (0–1).

Healthy adults (n = 22)				Older adults (n = 38)							
ID	Time	Weight	*BBS*/*BMI*	ID	Time	Weight	*BBS*/*BMI*	ID	Time	Weight	*BBS*/*BMI*
1	0.9883	0.9386	0.9681	23	0.7570	0.6803	0.3245	42	0.7874	0.8810	0.3830
2	0.9808	0.9695	0.9974	24	0.9676	0.8647	0.6808	43	0.8655	0.7978	0.5585
3	0.9781	0.9515	0.9389	25	0.9556	0.8203	0.6755	44	0.7114	0.6923	0.5293
4	0.9623	0.9462	0.9681	26	0.9600	0.8216	0.3245	45	0.9752	0.8251	0.9125
5	0.9837	0.9638	0.9389	27	0.9733	0.7008	0.7393	46	0.9685	0.8842	0.8950
6	0.9885	0.8221	0.9681	28	0.8888	0.8345	0.5585	47	0.8542	0.8922	0.7345
7	0.9842	0.9630	0.9974	29	0.9742	0.5937	0.7393	48	0.9123	0.8455	0.6212
8	0.9715	0.9660	0.9389	30	0.8366	0.8315	0.5585	49	0.7845	0.9121	0.5528
9	0.9864	0.8750	0.8856	31	0.4404	0.6366	0.6463	50	0.8867	0.8334	0.6852
10	0.9917	0.8755	0.9974	32	0.8986	0.7728	0.5000	51	0.8231	0.8762	0.5124
11	0.9780	0.8858	0.8856	33	0.7199	0.8501	0.6223	52	0.9412	0.8055	0.7825
12	0.9790	0.9150	0.9974	34	0.7893	0.8870	0.4415	53	0.8655	0.8211	0.6958
13	0.9730	0.8472	0.9734	35	0.7156	0.8712	0.5585	54	0.8998	0.9234	0.7123
14	0.9781	0.9120	0.9681	36	0.9061	0.8759	0.9096	55	0.7123	0.7245	0.3255
15	0.9903	0.8618	0.9681	37	0.7784	0.8123	0.5585	56	0.6844	0.6512	0.1458
16	0.9750	0.8504	0.9974	38	0.9283	0.8138	0.7341	57	0.7955	0.7544	0.4421
17	0.9842	0.7999	0.9149	39	0.9957	0.9073	0.8271	58	0.7422	0.7112	0.3845
18	0.9869	0.8157	0.9681	40	0.9700	0.9238	0.7926	59	0.9755	0.7321	0.5218
19	0.9919	0.9714	0.9681	41	0.8560	0.7301	0.1489	60	0.9682	0.7845	0.5582
20	0.9890	0.9440	0.9389								
21	0.9852	0.8923	0.9441								
22	0.9841	0.9520	0.9149								

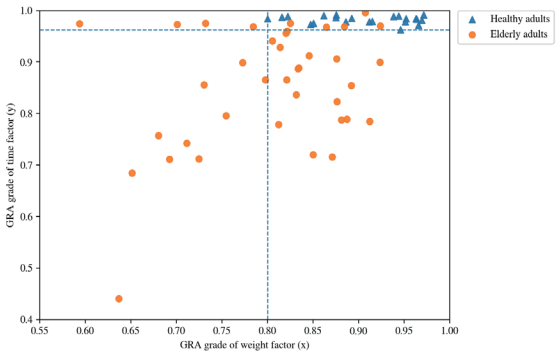

Fig. 3. (Color online) GRA grade distribution areas as a function of time and weight factors.

Table 4
Proportion of each group in the GRA grade distribution areas.

Areas	Older adults (n = 38)	Healthy adults (n = 22)
I	5 (13.2%)	22 (100.0%)
II	4 (10.5%)	0 (0.0%)
III	10 (26.3%)	0 (0.0%)
IV	19 (50.0%)	0 (0.0%)

Note: Quadrant numbering follows the standard Cartesian convention in Fig. 3: Area I (weight ≥ 0.7999, time ≥ 0.9623), Area II (weight < 0.7999, time ≥ 0.9623), Area III (weight < 0.7999, time < 0.9623), and Area IV (weight ≥ 0.7999, time < 0.9623).

weight < 0.7999) relative to the younger benchmark.[20] Finally, Area IV (50.0%, 19/38) represents "Stable Compensators". While these individuals maintain weight-shifting capability comparable to the younger norm (weight ≥ 0.7999), they show lower temporal efficiency (time < 0.9623). This profile suggests a "slow-but-stable" strategy in which movement speed is reduced to prioritize postural stability.[21]

4.2 Correlation of time efficiency with clinical indicators

The cross-analysis between movement speed and integrated clinical indicators (*BBS*/*BMI*) illustrates the limited sensitivity of traditional metrics in distinguishing multidimensional functional differences (Fig. 4, Table 5).[22] Using the healthy lower limits as thresholds (time = 0.9623; *BBS*/*BMI* = 0.8856), we categorized older adult participants into four areas. Area I represents the reference-like quadrant; however, only 5.3% (2/38) of older adults fell into this quadrant, suggesting that the concurrent maintenance of high temporal efficiency and high clinical stability is relatively uncommon in aging.[23] Area II accounts for 2.6% (1/38) and reflects a "clinically preserved but slower" profile, in which clinical indicators remain near the younger reference range while temporal efficiency is reduced. In contrast, Area III contains the majority of older adult participants (73.7%, 28/38), suggesting concurrent reductions in both temporal efficiency and *BBS*/*BMI*-related clinical stability.[24] Interestingly, 18.4% (7/38) of older adults are located in Area IV, suggesting that some individuals may preserve faster execution despite reduced clinical stability, possibly relying, to a greater extent, on momentum-related strategies to complete the transition.[25]

4.3 Impact of weight-shifting power on functional performance

The relationship between weight-shifting power and integrated clinical indicators (*BBS*/*BMI*) provides further insight into multidimensional functional differences (Fig. 5, Table 6).[26] Findings from Area I (7.9%, 3/38) suggest that only a small subset of older adults maintain weight-shifting capability comparable to the younger benchmark while also retaining high clinical stability. Interestingly, the absence of participants in Area II (0.0%) suggests that the combination of high *BBS*/*BMI*-related clinical stability and reduced weight-shifting power is uncommon in the present sample. Area III (36.8%, 14/38) represents a group characterized by concurrent reductions in both weight-shifting capability and clinical stability.[27] In contrast, the

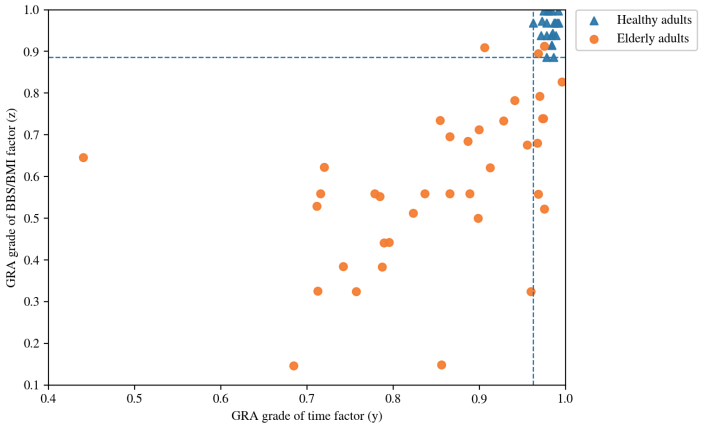

Fig. 4. (Color online) GRA grade distribution areas as a function of time factors and *BBS* & *BMI* factors. (Note: Some data points overlap due to identical coordinate values.)

Table 5
Proportion of each group in the GRA grade distribution areas.

Areas	Older adults (n = 38)	Healthy adults (n = 22)
I	2 (5.3%)	22 (100.0%)
II	1 (2.6%)	0 (0.0%)
III	28 (73.7%)	0 (0.0%)
IV	7 (18.4%)	0 (0.0%)

Note: Quadrant numbering follows the standard Cartesian convention in Fig. 4: Area I (time ≥ 0.9623, *BBS*/*BMI* ≥ 0.8856), Area II (time < 0.9623, *BBS*/*BMI* ≥ 0.8856), Area III (time < 0.9623, *BBS*/*BMI* < 0.8856), and Area IV (time ≥ 0.9623, *BBS*/*BMI* < 0.8856).

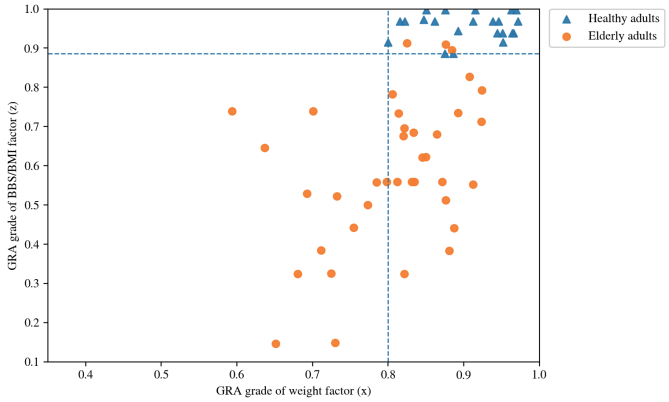

Fig. 5. (Color online) GRA grade distribution areas as a function of weight factors and *BBS* & *BMI* factors.

majority of older adults are located in Area IV (55.3%, 21/38), representing a relatively weight-preserved profile—individuals who retain comparatively high weight-shifting capability despite reduced clinical stability, which may reflect compensation through nonclinical movement strategies.

Table 6
Proportion of each group in the GRA grade distribution areas.

Areas	Older adults (n = 38)	Healthy adults (n = 22)
I	3 (7.9%)	22 (100.0%)
II	0 (0.0%)	0 (0.0%)
III	14 (36.8%)	0 (0.0%)
IV	21 (55.3%)	0 (0.0%)

Note: Quadrant numbering follows the standard Cartesian convention in Fig. 5: Area I (weight ≥ 0.7999, *BBS*/*BMI* ≥ 0.8856), Area II (weight < 0.7999, *BBS*/*BMI* ≥ 0.8856), Area III (weight < 0.7999, *BBS*/*BMI* < 0.8856), and Area IV (weight ≥ 0.7999, *BBS*/*BMI* < 0.8856).

4.4 Synthesis: 3D assessment norm as an integrative visual framework

The culmination of this research is the establishment of the Comprehensive 3D Graph of GRA grade distribution (Fig. 6), which serves as a multidimensional visual representation. As age progresses, the balance system of older adults may decline, posing significant challenges to maintaining postural stability and increasing the risk of traumatic injuries. While the results of previous 2D analyses provided essential insights into specific interactions (e.g., time vs. weight), they occasionally revealed overlapping performance ranges between certain older adult participants and the healthy young group, suggesting an apparent similarity in behavioral performance. However, as visualized in Fig. 6, the transition to a 3D space helps distinguish functional differences that are less apparent in lower-dimensional views.[28] For instance, in the 2D projection (time vs *BBS*/*BMI*), Participants 27 and 29 appear indistinguishable owing to identical clinical scores (0.7393) and nearly identical temporal grades (0.9733 vs 0.9742). However, they are clearly separable when the weight dimension is also considered (0.7008 vs 0.5937), suggesting that the 3D model may reveal functional differences that are less apparent in lower-dimensional assessments.

In the 3D functional space, the healthy young group forms a tight, high-performance reference cluster near the GRA coordinates of (1.0, 1.0, 1.0). This spatial distribution reflects the use of healthy young adults as the reference sequence in the present framework. In contrast, the 38 older adult participants are widely dispersed, suggesting heterogeneous age-related performance characteristics. This spatial dispersion may reflect variations in specific factor declines and possible compensatory adaptations—where one individual may drift as a result of temporal lags, and another may drift owing to force-shifting deficits. This visual distribution is consistent with the clinical concern regarding the lack of awareness among older adults; many may not readily perceive subtle changes in their own balance performance until functional decline becomes more evident.[29] By providing a standardized 3D visual platform, this model may serve as a "conceptual digital mirror," allowing both clinicians and older adults to more intuitively perceive the degree of functional drift from the healthy young reference baseline, thereby recognizing biomechanical differences that conventional observational scales might overlook and helping to inform future individualized assessment and movement-support strategies for fall prevention.[30]

Furthermore, the utilization of this 3D GRA distribution mechanism may offer advantages for future clinical scalability. By employing advanced mathematical techniques such as

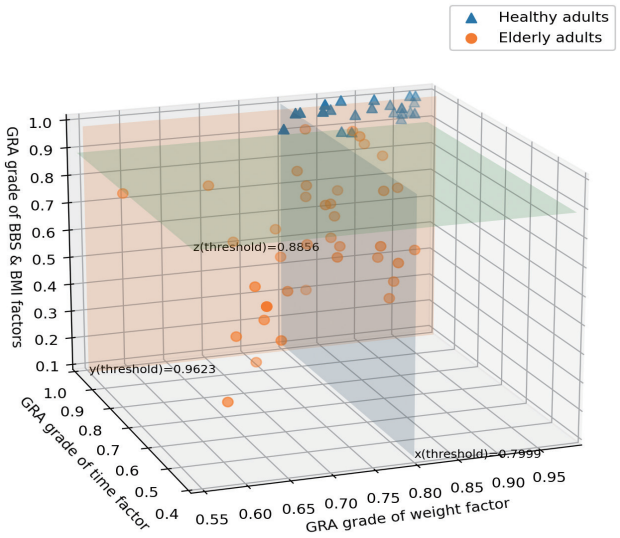

Fig. 6. (Color online) 3D graph of GRA grade distribution.

Euclidean distance from the high-performance reference cluster or multifactor regression analyses, it may be possible to estimate a relative "functional age" of a participant and further refine the assessment standards.[31] This approach may extend the framework beyond simple screening toward more individualized assessment and intervention planning, in which targeted strategies—such as reaction-time training or explosive power exercises—could be revealed by a participant's specific coordinates in the 3D space. Ultimately, this 3D assessment norm contributes to a more comprehensive understanding of geriatric balance and may provide a basis for the future integration of high-frequency sensors into AI-assisted smart home health monitoring and personalized fall-prevention systems.

5. Conclusions

In this study, we developed a reference-based 3D assessment norm for characterizing geriatric balance by integrating high-frequency (1000 Hz) force platform data with clinical parameters, including the *BBS* and *BMI*. By extracting 12 core biomechanical factors across temporal and weight-related dimensions and combining them with clinical indicators, the proposed model provides an interpretable multidimensional framework that may help address some limitations of traditional assessments, including their limited sensitivity to subtle functional differences. The findings suggest that older adults may exhibit different balance-related performance characteristics, including possible compensatory adaptations such as a relatively "slow-but-stable" profile identified through the joint consideration of temporal efficiency and clinical stability. The 3D visualization of these individual functional profiles—linking sensor-derived data with clinical profiles—may serve as a "conceptual digital mirror" that helps distinguish differences less apparent in lower-dimensional views. Ultimately, the

findings of this research will contribute to a more comprehensive understanding of geriatric balance and may provide a basis for future rehabilitation-oriented assessment and for the development of AI-assisted, multidimensional health monitoring systems for the aging population. Future longitudinal studies should include a further examination of the relationship between this 3D framework and external dynamic clinical measures, as well as fall-related outcomes, in order to refine its interpretability and potential clinical applicability.

Acknowledgments

This study was supported by a grant from the National Science Council (NSC 103-2221-E-431-007).

References

1 United Nations Department of Economic and Social Affairs, Population Division: World Population Prospects 2022: Summary of Results (United Nations Publications, New York, 2023). https://population.un.org/wpp/
2 M. Roig and D. Matsumoto: Economic Well-being at Older Ages: Prospects for the Future (United Nations Publications, New York, 2023). https://www.un.org/development/desa/ageing/
3 K. O. Berg, B. E. Maki, J. I. Williams, P. J. Holliday, and S. L. Wood-Dauphinee: Arch. Phys. Med. Rehabil. **73** (1992) 1073. https://pubmed.ncbi.nlm.nih.gov/1444775/
4 M. E. Tinetti, F. Williams, and R. Mayewski: Am. J. Med. **80** (1986) 429. https://doi.org/10.1016/0002-9343(86)90717-5
5 A. Yingyongyudha, V. Saengsirisuwan, W. Panichaporn, and R. Boonsinsukh: J. Geriatr. Phys. Ther. **39** (2016) 64. https://doi.org/10.1519/JPT.0000000000000050
6 S. T. Hung, Y. C. Cheng, C. C. Wu, and C. H. Su: J. Multidiscip. Healthc. **16** (2023) 1889. https://doi.org/10.2147/JMDH.S419306
7 M. Jalali, P. Mojgani, H. Saeedi, F. Azadinia, M. Niksolat, and F. Ghorbani: Int. J. Older People Nurs. **16** (2021) e12412. https://doi.org/10.1111/opn.12412
8 M. H. Gerards, R. G. Marcellis, M. Poeze, A. F. Lenssen, K. Meijer, and R. A. de Bie: BMC Geriatr. **21** (2021) 5. https://doi.org/10.1186/s12877-020-01944-7
9 K. Honda, Y. Sekiguchi, A. Sasaki, K. Handa, Y. Nakamura, and T. Tateuchi: J. Biomech. **129** (2021) 110813. https://doi.org/10.1016/j.jbiomech.2021.110813
10 E. Stolz, A. Schultz, J. Zuschnegg, F. Großschädl, T. E. Dorner, R. Roller-Wirnsberger, and W. Freidl: Eur. J. Ageing **21** (2024) 28. https://doi.org/10.1007/s10433-023-00792-9
11 E. Javanmardi, S. Liu, and N. Xie: Systems **11** (2023) 70. https://doi.org/10.3390/systems11020070
12 J. Deng: J. Grey Syst. **1** (1989) 1. https://uranos.ch/research/references/Julong_1989/10.1.1.678.3477.pdf
13 B.-L. Jian, C.-C. Wang, H.-T. Yau, L.-W. Wu, and A.-H. Tian: Sensors and Materials **32** (2020) 843. https://doi.org/10.18494/SAM.2020.2674
14 S. Javed, A. Khan, W. Dong, A. Raza, and S. Liu: Processes **7** (2019) 348. https://doi.org/10.3390/pr7060348
15 C. S. Chang: Axioms **10** (2021) 341. https://doi.org/10.3390/axioms10040341
16 Y. C. M. Lor, M. T. Tsou, L. W. Tsai, and S. Y. Tsai: BMC Geriatr. **23** (2023) 421. https://doi.org/10.1186/s12877-023-04012-y
17 L. Piano, T. Geri, and M. Testa: Arch. Physiother. **10** (2020) 9. https://doi.org/10.1186/s40945-020-00078-8
18 D. B. Jepsen, K. Robinson, G. Ogliari, M. Montero-Odasso, N. Kamkar, J. Ryg, E. Freiberger, and T. Masud: BMC Geriatr. **22** (2022) 446. https://doi.org/10.1186/s12877-022-03271-5
19 S. Sadeh, D. Gobert, K.-H. Shen, F. Foroughi, and H.-Y. Hsiao: Clin. Biomech. **109** (2023) 106068. https://doi.org/10.1016/j.clinbiomech.2023.106068
20 S. M. Aloraini, A. A. Abu Mismar, H. F. Aloqaily, K. A. Alghadir, and S. A. Alharethy: Phys. Ther. Rev. **28** (2023) 1. https://doi.org/10.1080/10833196.2023.2168850
21 O. E. Svinøy, G. Hilde, A. Bergland, and B. H. Strand: Clin. Interv. Aging **16** (2021) 335. https://doi.org/10.2147/CIA.S294512
22 F. Migliorini, R. Giorgino, F. Hildebrand, A. S. Brydone, and N. Maffulli: Medicina (Kaunas) **57** (2021) 1119. https://doi.org/10.3390/medicina57101119

23 J. Aunger and G. Wagnild: Am. J. Hum. Biol. **34** (2022) e23546. https://doi.org/10.1002/ajhb.23546
24 B. C. L. So, M. M. Y. Kwok, N. W. L. Lee, W. Y. Ho, and I. K. K. Cheung: Healthcare (Basel) **11** (2023) 441. https://doi.org/10.3390/healthcare11030441
25 F. Sigrist, A. Oliveira, and H. Fichman: Dement. Neuropsychol. **15** (2021) 366. https://doi.org/10.1590/1980-57642021dn15-030014
26 L. H. S. Soh, C. W. Tan, J. I. Thomas, and P. D. Whitehead: J. Frailty Sarcopenia Falls **6** (2021) 131. https://doi.org/10.22540/JFSF-06-131
27 B. Kaambwa, N. Bulamu, C. Mpundu-Kaambwa, and R. Oppong: Int. J. Environ. Res. Public Health **18** (2021) 10314. https://doi.org/10.3390/ijerph181910314
28 C. Y. Huang, Y. C. Lin, Y. C. Lu, P. C. Chen, and C. L. Liu: Brain Sci. **12** (2022) 1642. https://doi.org/10.3390/brainsci12121642
29 T. Jian: Healthcare (Basel) **11** (2023) 42. https://doi.org/10.3390/healthcare11010042
30 S. Liu and N. Xie: Grey Information: Theory and Practical Applications (Springer, Singapore, 2022). https://doi.org/10.1007/1-84628-342-6_5
31 H. W. Jung, T. Jin, J. Y. Baek, S. Yoon, E. Lee, J. M. Guralnik, and I. Y. Jang: Clin. Interv. Aging **15** (2020) 2175. https://doi.org/10.2147/CIA.S280542

About the Authors

Chih Sheng Chang received his Ph.D. degree from the Institute of Design Science, Tatung University, Taipei, Taiwan, in 2011. He is now an associate professor in the Department and Graduate School of Product and Media Design, Fo Guang University. His research interests include product design, ergonomics, grey system theory applications, and kansei engineering. (cschang@mail.fgu.edu.tw)

Ke Shin Chong received her M.S. degree from the Department of Product and Media Design, Fo Guang University, Yilan, Taiwan, in 2023. Her research interests include product design, media design, graphic design, and ergonomics. (Kitty.chong1011@gmail.com)